

## Mutual inhibition of the dimerized Na/Ca-K exchanger in rod photoreceptors

Paul J. Bauer \*, Heike Schauf

*Institute for Biological Information Processing (IBI-1), P.O. Box 1913, Research Center Juelich, D-52425 Juelich, Germany*

Received 19 July 2001; received in revised form 12 November 2001; accepted 22 November 2001

---

### Abstract

In the dark, rod photoreceptors sustain a continuous influx of Na and Ca ions through the cGMP-gated channels of the rod outer segments (ROS). Whereas Na ions are extruded in the inner segment by the Na-pump, Ca ions are extruded already in the ROS by Na/Ca-K exchange. Our previous findings indicate that in the ROS plasma membrane, exchanger and channel form a complex of two exchangers associated per channel [1,2]. Here, we report evidence of a novel regulatory mechanism of the dimerized exchanger, based on the following findings: (1), thiol-specific cross-linking with dimaleimides resulted in an increase of the Na/Ca-K exchange activity which correlated with the size of the cross-linking reagent, i.e., with increasing separation of the monomers in a dimerized exchanger; (2), partial proteolysis of the exchanger also increased the exchange rate by about a factor of two; (3), disintegration of the channel-exchanger complex by solubilization of the ROS membranes and preparation of proteoliposomes resulted in a twofold enhancement of the exchange rate; however (4), partial proteolysis of proteoliposomes, in which the exchanger molecules exist as monomers, did not result in any enhancement of the exchange rate. These findings suggest an inhibitory protein domain at the contact site of the dimerized exchanger. The physiological implication of this inference will be discussed in terms of a potential allosteric regulation of the exchanger in the channel-exchanger complex. © 2002 Elsevier Science B.V. All rights reserved.

**Keywords:** Na–Ca exchange; Regulation; cGMP gated channel; Local Ca signaling; Cross-linking; Proteolysis

---

### 1. Introduction

In the rod outer segments (ROS) of photoreceptors, the cytosolic Ca concentration is determined by Ca influx through cGMP-gated channels and by Ca extrusion via Na/Ca-K exchange [3–6]. Both cGMP-gated channels and Na/Ca-K exchangers are localized exclusively in the plasma membrane of the ROS [7–9]. There is evidence that retinal cGMP-gated channels function as tetrameric proteins [10–

13] whereas retinal Na/Ca-K exchangers are active as monomers [14]. In the plasma membrane of the ROS, however, the exchanger is likely to exist in the dimerized state [1].

In the dark, cGMP-gated channels mediate a continuous cation current into the ROS consisting of Na ions (80%), Ca ions (15%), and Mg ions (5%) [15]. Upon light absorption, cGMP is rapidly hydrolyzed and the cGMP-gated channels close, thus interrupting the cation influx while Ca extrusion continues. The resulting decrease in cytosolic Ca concentration plays an important role in mediating the recovery of the dark state of the photoreceptor as well as in light adaptation (reviewed in [16]).

---

\* Corresponding author. Fax: +49-2461-614216.  
E-mail address: p.j.bauer@fz-juelich.de (P.J. Bauer).

Na/Ca-K exchange in rod photoreceptors has been extensively studied, however, not much is known on a possible regulatory mechanism. Based on Ca-flux experiments in ROS suspensions, Schnetkamp et al. suggested that intradiscal Ca plays an inhibitory role for Na/Ca-K exchange of the ROS [17]. However, this hypothesis could not be further substantiated due to the difficulty in determining intradiscal Ca [18,19]. Also, a Ca transport protein in the disc membranes has yet to be unequivocally identified.

Similar to other Na–Ca exchangers, the activity of the Na/Ca-K exchanger may be controlled by some protein domain of the exchanger itself because partial proteolysis enhances the rate of Na/Ca-K exchange [20–22]. An endogenous inhibitory domain, the so-called XIP region, has been identified in the intracellular loop of the cardiac Na–Ca exchanger [23]. However, there is very little sequence homology between both types of exchangers; in particular, the Na/Ca-K exchanger of rod photoreceptors contains no protein domain similar to the XIP domain of the cardiac Na–Ca exchanger [24].

Recently, we reported evidence indicating that in bovine ROS plasma membranes the Na/Ca-K exchanger is associated with the cGMP-gated channel [2,14]. Furthermore, thiol-specific cross-linking indicated that two exchanger molecules bind per channel [1]. Here, we examine the influence on the exchange rate of thiol-specific cross-linking and of partial proteolysis of the exchanger. The results indicate a putative regulatory mechanism based on dimerization of the exchanger. A short account of this work has recently been presented to the Biophysical Society [25].

## 2. Materials and methods

### 2.1. Purification of bovine rod outer segments

Bovine retinas were prepared from cattle eyes collected in a local slaughter house. Rod outer segment (ROS) were purified as described earlier [7]. Aliquots of purified ROS, containing 5 or 10 mg of rhodopsin, were shock-frozen in 600 mM sucrose and stored at  $-80^{\circ}\text{C}$  until use. All preparations were carried out in dim red light.

### 2.2. Preparation of rod outer segment membrane vesicles

Purified ROS containing 20 mg of rhodopsin were defrosted, hypotonically lysed in 0.5 mM Tris, 0.5 mM HEPES, 1 mM EDTA, 1 mM DTT and pelleted for 30 min at  $48\,000\times g$  and  $4^{\circ}\text{C}$ . This washing step was repeated in the absence of DTT, the pellet was resuspended in 100 mM KCl and 10 mM HEPES adjusted to pH 7.4 with KOH (K-HEPES), and the suspension was pelleted for 15 min at  $27\,000\times g$  and  $4^{\circ}\text{C}$ . The pellet was then resuspended in 2 ml K-HEPES and, for reasons given below, shock-frozen in liquid nitrogen to obtain fused ROS membranes. The sample was then thawed, the volume increased to 4 ml by addition of K-HEPES, and 10 mM  $\text{CaCl}_2$  were added. To prepare ROS membrane vesicles, the suspension was slightly homogenized by passing it through a syringe, and then forcing it first through a  $1\text{-}\mu\text{m}$ , then through a  $0.4\text{-}\mu\text{m}$  Nuclepore filter.

It should be noted that without freeze-thawing, the Na-induced Ca release from ROS membrane vesicles was rather small because of the fact that the exchanger is localized exclusively in the plasma membrane, which constitutes only about 6% of the total membrane area of the bovine ROS membranes [7,9]. Fusion of ROS disk and plasma membranes was achieved by the above described freeze-thawing protocol, and led to vesicle preparations with an almost tenfold higher Na-induced Ca release as compared to non-fused membrane vesicles [14].

### 2.3. Thiol-specific cross-linking

All preparation steps were carried out in dim red light. For cross-linking studies, the extruded ROS membrane vesicles were divided into two aliquots of equal volumes. To one aliquot that served as a control, 2 mM DTT was added. The second aliquot was cross-linked at room temperature as follows. To cleave possible disulfide bridges, 50  $\mu\text{M}$  DTT was first added, then 100  $\mu\text{M}$  of the cross-linking reagent from a freshly prepared 10 mM stock solution in dimethyl sulfoxide (DMSO) was added. The reaction was stopped after 10 min by addition of 2 mM dithiothreitol (DTT). The thiol-specific cross-linking reagents were (in parentheses: abbreviation and

spacer arm length): ortho-phenylidene dimaleimide (oPDM, 4.98 Å), para-phenylidene dimaleimide (pPDM, 11.4 Å), 1,3-bis-maleimido-propane (BMP, 9.6 Å), 1,6-bis-maleimido-hexane (BMH, 16.1 Å), 1,4-bis-maleimidyl-2,3-dihydroxybutane (BMDB, 10.9 Å), and the mono-functional cysteine modifying reagent, *N*-ethylmaleimide (NEM). Cross-linking with 1,10-phenanthroline-complexed copper (CuPhe) was carried out as described [1] except that the reaction was not stopped with EDTA, but instead by removing Cu ions along with Ca ions with K-Chelex-100 (see below). BMP was synthesized by Dr. V. Hagen (FMP Berlin, Germany), BMDB and BMH was purchased from Pierce, and all other reagents were purchased from Sigma.

#### 2.4. Preparation of proteoliposomes

Hypotonically washed ROS membranes, containing 15 mg rhodopsin, were solubilized at 4°C for 30 min in 24 ml of 12 mM CHAPS, 150 mM KCl, 0.5 mM CaCl<sub>2</sub>, 1 mM DTT, 10 mg/ml soybean phosphatidylcholine, and 10 mM HEPES adjusted with KOH to pH 7.4. After centrifugation for 30 min at 4°C and 48 000×*g*, the supernatant was dialyzed at 4°C for 40 h against 2 l of 100 mM KCl, 2 mM CaCl<sub>2</sub>, 10 mM HEPES adjusted with KOH to pH 7.4, replacing the dialysis buffer four times.

#### 2.5. Partial proteolysis

Proteolysis was carried out by addition of 1 µg/ml trypsin to the membrane vesicles or proteoliposomes. The temperature was kept constant at 25°C with a water bath. After 1 h of trypsin incubation, proteolysis was terminated by addition of an 20-fold excess of soybean trypsin inhibitor (Sigma).

#### 2.6. Ca-flux assay and determination of initial Ca-fluxes

Immediately before the measurement, non-included Ca was removed by passage of the vesicle suspension through 1 ml of the ion exchange resin K-Chelex-100 (BioRad, mesh 200–400), using a Swinnex-13 filter holder (Millipore) with a 3-µm pore size Nuclepore filter fitted to a syringe. Arse-

nazo III was added to a final concentration of 50 µM and the absorbance difference between 652 and 700 nm recorded in a dual wavelength spectrophotometer (Aminco DW 2000) using an OS-119.004 cuvette (Hellma). The suspension was stirred in the cuvette with a magnetic bar, and the temperature was kept constant at 25°C. A small port fitting a Hamilton syringe was mounted on the spectrophotometer to add solutions without removing the cuvette. After the Ca-flux assay, the protein content of each sample was determined according to the Amido Black procedure [26].

To determine the initial Na-induced Ca-flux, the tangent of the Ca-flux curve has to be obtained at time zero, i.e., the time of Na-addition. Unfortunately, there is an unavoidable injection artifact due to the finite mixing period which lasts for 1–2 s. Therefore, the Ca-flux curve was fitted between 3 and 30 s after addition of Na with a quadratic regression curve, and extrapolated to time zero to obtain the slope of the Ca-flux at time zero. The Ca-flux due to passive Ca-leakage was determined by the slope of a linear regression of the data recorded 120 s before addition of Na. The difference between these two fluxes is denoted the initial Na-induced Ca-flux. The conversion from OD-values to Ca-concentrations is described in the legend to Fig. 2.

#### 2.7. Protein analysis

After solubilization of the proteins in 1.6% sodium dodecyl sulfate in the presence of 5% β-mercaptoethanol, electrophoresis was carried out on a 3.5%–7.5% polyacrylamide gel (SDS–PAGE). The proteins were then electro-eluted onto a polyvinylidene difluoride membrane (PVDF membrane, Immobilon P, Millipore) and labeled with monoclonal antibodies, as described previously [1]. The protein content of vesicle suspensions was determined according to the Amido Black procedure [26]. The rhodopsin concentration was determined spectroscopically from the absorbance difference at 500 nm between non-bleached and bleached ROS membranes upon solubilization in 2% Emulphogene BC-720, using an extinction coefficient of 40 000 M<sup>-1</sup> cm<sup>-1</sup>.

### 2.8. Influence of vesicle size on the Ca-efflux kinetics, and determination of Ca-flux and Ca-permeability independent of the vesicle geometry

In the following, it will be shown that generally the Ca-efflux kinetics of spherical vesicles depends on the size of the vesicles. However, the initial rate of efflux does not depend on the vesicles geometry and can be used to determine the membrane permeability if the vesicle diameter is known.

Assume a homogeneous ensemble of spherical vesicles containing an ion concentration  $c$  which is much higher than the external concentration of this ion (which, in our case, is Ca). If the permeability of the membrane is suddenly increased at time zero (for instance, by activating the exchanger or the cGMP-gated channel), then the intravesicular ion concentration decreases according to

$$\frac{dc}{dt} = -kc \quad (1a)$$

i.e., according to the single-exponential law,

$$c = c_0 \cdot e^{-kt} \quad (1b)$$

where the rate constant,  $k$ , is a function of the membrane permeability and the vesicle geometry. This is readily seen by introducing the membrane permeability,  $P$ , according to

$$j = -P\Delta c \quad (2a)$$

where  $j$  is the ion flux per unit area, and  $\Delta c$  denotes the concentration difference between intra- and extracellular ions. Assuming that the extravesicular ion concentration is negligible, we obtain

$$j = -Pc \quad (2b)$$

Hence, the total flux at some time,  $J(t)$ , from  $N$  vesicles of the surface area,  $Na$ , is

$$J(t) = -NaPc(t) \quad (31)$$

The initial ion flux,  $J_0$ , at time zero is given by

$$J_0 = -NaPc_0 \quad (3b)$$

which depends only on the total membrane area,  $Na$ , and the ion concentration,  $c_0$ , at time zero. In particular,  $J_0$  is independent of the vesicle geometry because decreasing the vesicle size,  $a$ , would entail a corre-

sponding increase in the number of vesicles,  $N$ . If there are  $n$  moles of ions in each vesicle of volume,  $v$ , then  $c(t) = n(t)/v$ , and the total flux  $J(t)$  is given as

$$J(t) = N \frac{dn}{dt} \quad (4)$$

Hence, we obtain by differentiation of Eq. 3a the differential equation

$$\frac{dJ}{dt} = -\frac{a}{v}PJ \quad (5a)$$

with the solution

$$J = J_0 e^{-k(r)t} \quad (5b)$$

where the rate constant,  $k$ , is given as

$$k(r) = \frac{a}{v}P \quad (6a)$$

and for spherical vesicles of radius,  $r$ , is

$$k(r) = \frac{3P}{r} \quad (6b)$$

Therefore, the kinetics of the ion efflux depends on the geometry of the vesicles. If spherical vesicles are distributed according to the distribution function,  $D(r)$ , with

$$\int D(r)dr = 1 \quad (7)$$

Eq. 5b has to be generalized to

$$J = J_0 \int D(r)e^{-k(r)t}dr \quad (8a)$$

Therefore, the efflux is not single-exponential because of the size distribution of vesicles. With regard to Eq. 7, this equation yields for the time  $t=0$

$$J = J_0 \quad (8b)$$

which means that the initial flux is also in this more general case independent of the geometry of the vesicles. Integration of Eq. 8a over time, and considering Eq. 6b yields the total ion release

$$\int_0^\infty Jdt = \frac{J_0 \langle r \rangle}{3P} \quad (9a)$$

where the mean vesicle radius is given by

$$\langle r \rangle = \int r D(r) dr \quad (9b)$$

According to Eq. 9a, the permeability can be obtained from the total ion release,  $\int_0^\infty J dt$ , and the initial flux,  $J_0$ ,

$$P = \frac{J_0 \langle d \rangle}{6 \int_0^\infty J dt} \quad (10)$$

if the mean diameter of the vesicles,  $d$ , is used instead of the radius.

### 3. Results

#### 3.1. Thiol-specific cross-linking

In the rod outer segments (ROS) of vertebrate photoreceptors, the Na/Ca-K exchanger can readily be cross-linked with thiol-specific reagents to form dimers indicating that this protein exists as a dimer in the membrane [1]. Presumably, only one or two cross-links form since only 6 out of the 1199 amino acids of the Na/Ca-K exchanger are cysteines [24]. We used thiol-specific reagents of different sizes to determine the distance between the adjacent cysteines which were cross-linked. Fig. 1 shows that a significant fraction of exchanger was cross-linked in ROS membranes with different dimaleimides having spacer lengths between 5 Å and 16 Å. In each cross-link experiment, the dimer band of the exchanger at 490 kDa is clearly visible while a significant fraction of monomeric exchanger at 250 kDa is apparent as well. Moreover, there are several fragment bands of the exchanger, mainly at 150 and 80 kDa, and a cross-link band at 420 kDa which is due to a cross-link between the monomer exchanger and the 150 kDa exchanger fragment [1].

The finding that thiol-specific cross-linking reagents with quite different spacer arms yield exchanger dimers indicates that there is a significant fluctuation of the distance between adjacent cysteines, probably due to thermal motion. Nevertheless, the cross-link should impose mechanical strain on the exchanger dimer if the size of the cross-linker does not match exactly the mean distance between the

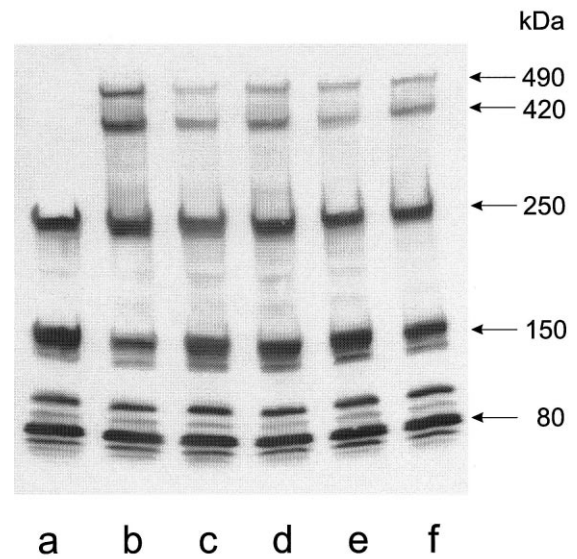


Fig. 1. Thiol-specific cross-linking of fused ROS membranes with dimaleimides. The membrane proteins were analyzed by SDS-PAGE and blotted onto a PVDF-membrane. The blot was labeled with the monoclonal antibody PMe 1B3 against the Na/Ca-K exchanger. As a control, non-cross-linked membranes are shown in lane a. Lanes b–f show membranes cross-linked with: b, BMH (spacer length 16.1 Å); c, BMDB (10.9 Å); d, BMP (9.6 Å); e, pPDM (11.4 Å); f, oPDM (4.98 Å). The monomer band of the exchanger is at 250 kDa, the dimer band at 490 kDa. The bands below 250 kDa are fragmental bands of the exchanger, the band at 420 kDa is due to a cross-link of the monomeric exchanger with a fragmental band [1]. It should be noted that the transfer efficacy of the electro-elution decreases for increasing molecular masses.

adjacent cysteines. Therefore, we investigated whether thiol-specific cross-linking of the exchanger influences the Na/Ca-K exchange, and more specifically, whether the size of the cross-linking reagent influenced the rate of Na/Ca-K exchange.

To answer this question, we examined the Na-induced Ca efflux from Ca-loaded vesicles made of ROS membranes which were cross-linked with thiol-specific reagents. Ca-loaded vesicles were prepared by extrusion of fused ROS membranes through Nuclepore filters, as described in the Section 2. After removal of the external Ca, Na ions induced similar Ca-fluxes from both vesicles of ROS membranes which were cross-linked with the dimaleimide pPDM, and from non-treated membranes (Fig. 2A,B). For comparison, the recordings were shifted in ordinate direction so as to start at the same point after the Na-addition. The downward deflections

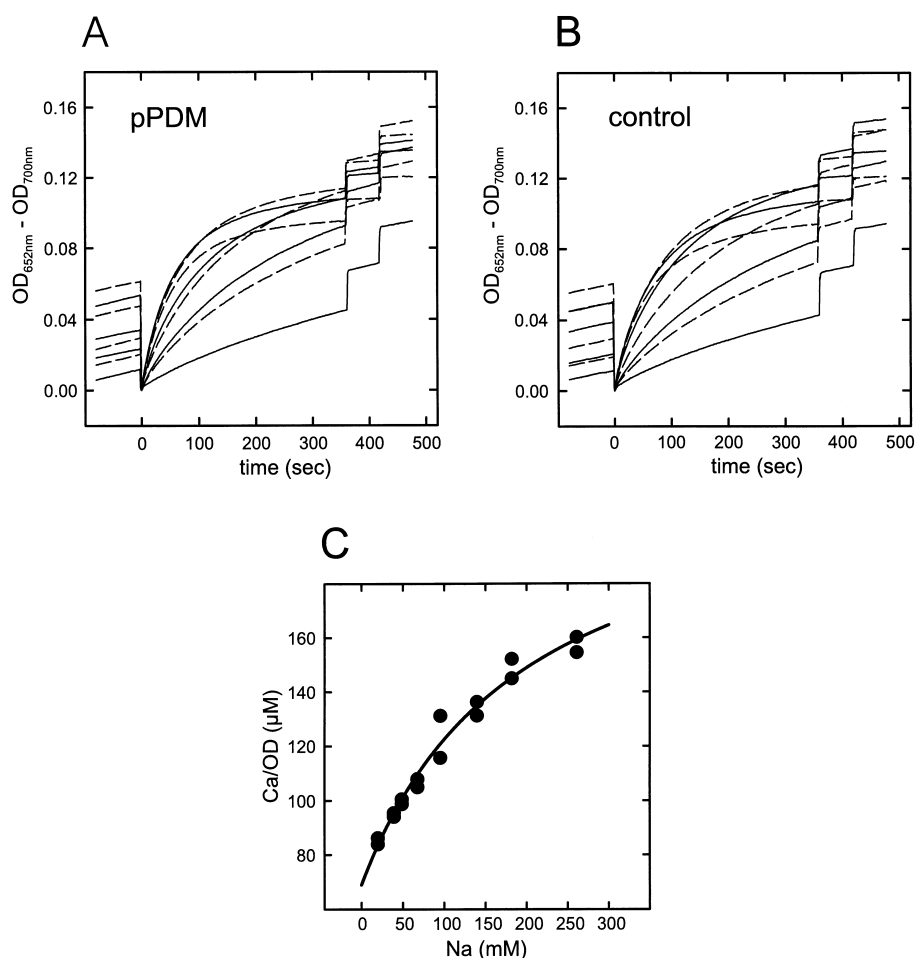
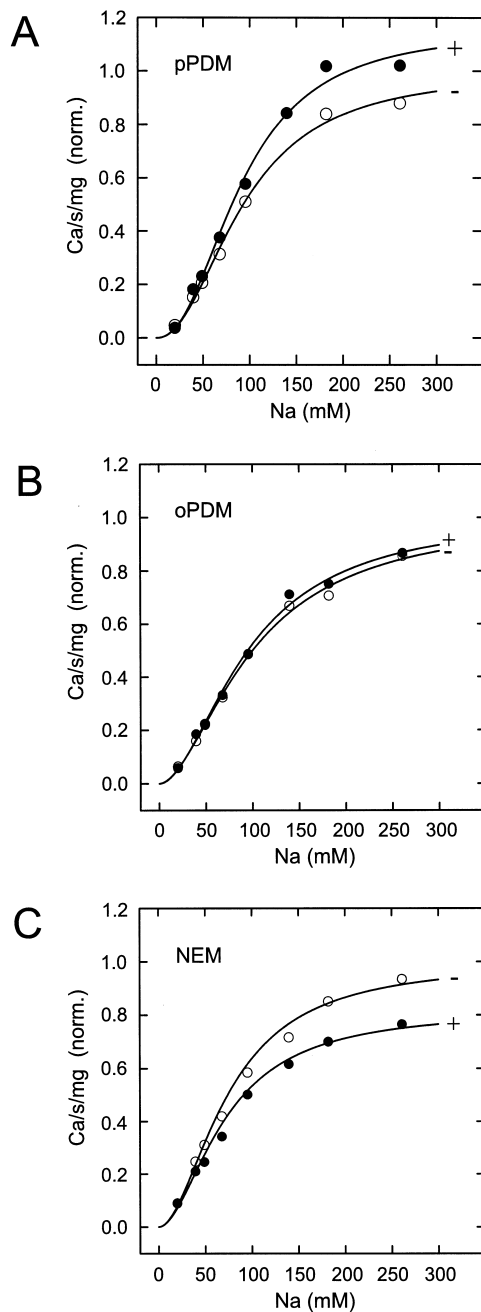


Fig. 2. Na-induced Ca-fluxes from ROS membrane vesicles: (A) after cross-linking with pPDM, and (B) without cross-linking (control). The following Na-concentrations were added at time zero (final concentrations in mM): 19.8, 39.2, 48.8, 67.6, 95.2, 140, 182, 261. The curves are alternately plotted with solid and dashed lines. For comparison, the recordings are shifted deliberately in ordinate direction such that the Ca release after Na-addition starts at zero. The downward deflection upon Na-addition is due to a reduction of the Ca-affinity of arsenazo III in the presence of Na (C); thus, the amplitude of this effect depends on both the Na- and the Ca-concentration. The increase of Ca-concentration due to passive leakage was  $8.9 \pm 1.8$  and  $8.2 \pm 1.7$  nM/s for pPDM-treated and control membrane vesicles, respectively. In C, the factor,  $\Delta Ca/\Delta OD$ , to convert the OD signal into a change of Ca-concentration is plotted as a function of the Na-concentration. These factors were determined for each experiment, by injecting twice, 6 min after the Na-addition, 2  $\mu$ l of a 1 mM  $CaCl_2$  solution (cf. A,B). A quadratic regression curve through the data is drawn as a solid line. An increase of the conversion factor  $\Delta Ca/\Delta OD$  means a decrease in the Ca-sensitivity of arsenazo III.

upon adding NaCl were due to Na-dependent decreases of the Ca-sensitivity of the indicator, arsenazo III [27]. To convert absorbance changes into Ca-concentration changes, standard pulses of  $CaCl_2$  were added 6 min after the addition of NaCl. The conversion factor,  $\Delta Ca/\Delta OD$ , increased significantly with increasing Na-concentration due to decreased Ca-sensitivity of arsenazo III (Fig. 2C). The decrease of the absorption signal of arsenazo III with increasing Na-concentration is also apparent from the

asymptotic values of the original recordings shown in Fig. 2A,B, which are clearly smaller for the highest Ca-concentrations. The recordings have the same asymptote when the data are converted into changes of Ca-concentration using the appropriate conversion factors,  $\Delta Ca/\Delta OD$  (not shown).

The data shown in Fig. 2 indicate that thiol-specific cross-linking did not markedly interfere with the transport function of the exchanger. This is remarkable because covalent protein modification is likely



to be detrimental. Surprisingly, a quantitative evaluation of the recordings revealed that cross-linking with pPDM even enhanced the Na–Ca exchange. Upon cross-linking with pPDM, the maximal initial Ca-efflux from fused ROS membrane vesicles was enhanced by about 12% as compared with non-treated vesicles, whereas the  $EC_{50}$ -value and the Hill coefficient were unchanged (Fig. 3A). The en-

Fig. 3. Initial Na-induced Ca-fluxes from ROS membrane vesicles: comparison of cross-linked and non-cross-linked membranes. (A) Thiol-specific cross-linking with pPDM (spacer length 11.4 Å); (B) the isomer oPDM (spacer length 4.98 Å). (C) The influence of NEM modification of cysteines on the initial Ca-flux. In every panel, the data obtained from the cross-linked and NEM-modified membranes, respectively, are plotted with filled circles, whereas the non-modified membranes are shown with open circles. The data are fitted with Hill curves, labeled with a plus sign for cross-linked or NEM-treated membrane vesicles, and labeled with a minus sign for chemically unmodified membrane vesicles. The data are normalized so that the Hill curve for the control values (labeled with a minus sign) approaches the asymptote one.

hancement of the rate of the Na–Ca exchange by thiol-specific cross-linking was virtually absent for oPDM, an analogous reagent with a much shorter spacer arm of 4.98 Å as compared to 11.4 Å for pPDM (Fig. 3B). On the other hand, simple alkylation of the cysteines of the exchanger with NEM had the opposite effect, leading to a distinct decrease of the maximal exchange rate, as one would expect (Fig. 3C).

These findings suggested that variation of the distance of the dimerized exchanger molecules by cross-linking with reagents of different size influenced the rate of Na–Ca exchange. We examined this hypothesis further by cross-linking with various dimaleimides and by disulfide bridging of the adjacent cysteines. Cross-linking with bismaleimidohexane, a reagent with a 16.1 Å spacer arm, resulted in a significant enhancement of the Na–Ca exchange. The enhancement of the Na-induced Ca-efflux upon cross-linking with BMDB was similar to pPDM, both reagents having also similar spacer arms (10.9 and 11.4 Å, respectively). On the other hand, direct cross-linking of the adjacent cysteines of the exchanger by a disulfide bridge resulted in the opposite effect, i.e., in a significant decrease of the Na–Ca exchange (Fig. 4).

A quantitative evaluation of these cross-linking results is shown in Fig. 5. For ROS membrane vesicles cross-linked with dimaleimides, the maximal Na-induced Ca-effluxes were divided by the maximal Ca-efflux obtained from NEM modified vesicles to account for the inhibitory effect of the NEM modification. For membrane vesicles cross-linked with disulfide bridges (i.e., treated with CuPhe), the maximal

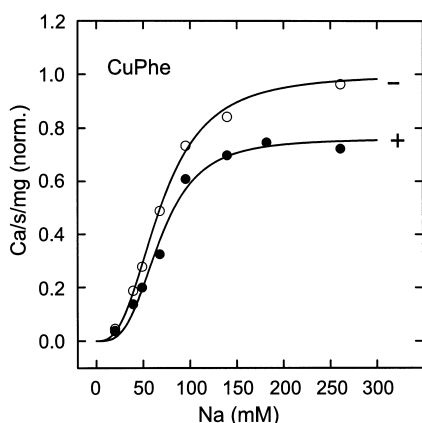


Fig. 4. Influence of disulfide bridging of ROS membranes on the initial Na-induced Ca-flux. Oxidation of the cysteines to disulfides was carried out with CuPhe and stopped by removal of Cu ions along with the Ca ions, immediately before the Ca-release experiment. The control membranes vesicles contained 2 mM DTT. The data are fitted with Hill curves and normalized, as described in the legend of Fig. 3.

Na-induced Ca-efflux was divided by the maximal Ca-efflux from non-treated membrane vesicles. Plotting these ratios of Ca-fluxes against the spacer arm of the thiol-specific reagent yields a clear dependence of the size of the reagent with the enhancing, or inhibitory influence on the exchanger (Fig. 5). A cubic regression curve through the data indicates that no effect is expected if the cross-linker has a spacer arm of 3 Å, suggesting that this is the mean distance of the adjacent cysteines (Fig. 5, dotted line). The maximal Na-induced Ca flux of the control samples (i.e., non-modified ROS membranes) was  $0.059 \pm 0.012$  mol  $\text{Ca}^{2+}/\text{s}$  per mol Rh ( $n = 13$ ).

These cross-linking experiments indicate that increasing the distance between the two molecules of the exchanger dimer with a cross-linker enhances the exchanger activity whereas tightening the exchanger contact by a disulfide bridge is inhibitory. Therefore, the contact side of the exchanger dimer may contain an endogenous protein domain which leads to mutual inhibition of the exchanger activity. Can the exchange activity be enhanced by cutting off this inhibitory domain?

### 3.2. Partial proteolysis

It has been reported that partial proteolysis enhances the activity of the rod Na/Ca-K exchanger, indi-

cating that an inhibitory protein domain can be clipped off by proteolysis [21,22]. Is this inhibitory domain the contact site between two monomers? If so, proteolysis should have no effect on the exchange rate if the exchanger is not dimerized.

We solubilized the ROS membranes in CHAPS in order to disintegrate the channel-exchanger complex. After addition of lipids, proteoliposomes were prepared by dialysis. Previously, we reported that upon reconstitution into liposomes, the exchangers cannot be cross-linked with thiol-specific reagents, indicating that the exchanger does not exist as a dimer in this preparation [1]. Therefore, a mutual interaction between the exchanger molecules can be excluded in this preparation. Can the exchanger still be activated by partial proteolysis?

Fig. 6B shows the Na-induced Ca-fluxes from ROS proteoliposomes elicited at about half-maximal exchanger activation. The Ca-fluxes from proteolytically treated proteoliposomes and non-trypsinized

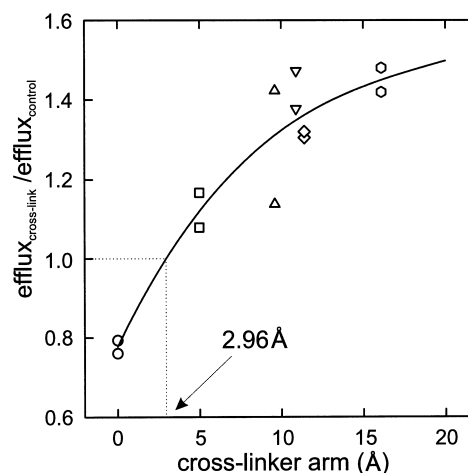


Fig. 5. Influence of the spacer length of the cross-linking reagent on the exchange rate. The ratios of the initial Ca-fluxes of the cross-linked membrane vesicles and the corresponding control membranes were calculated. For the dimaleimides oPDM ( $\square$ ), BMP ( $\triangle$ ), BMDDB ( $\nabla$ ), pPDM ( $\diamond$ ), and BMH ( $\circ$ ), the NEM-modified membrane vesicles were taken as the appropriate control membranes, to account for the inhibitory influence of the NEM-modification of these cross-linkers (cf. Fig. 3C). For disulfide bridged membranes ( $\circ$ ), non-modified ROS membranes in the presence of 2 mM DTT were taken as the control membranes. The solid line is a cubic regression curve through the data. The ordinate value of 1 attained by the regression curve for the spacer length 2.96 Å presumably reflects the distance of the adjacent cysteines leading to the cross-link.



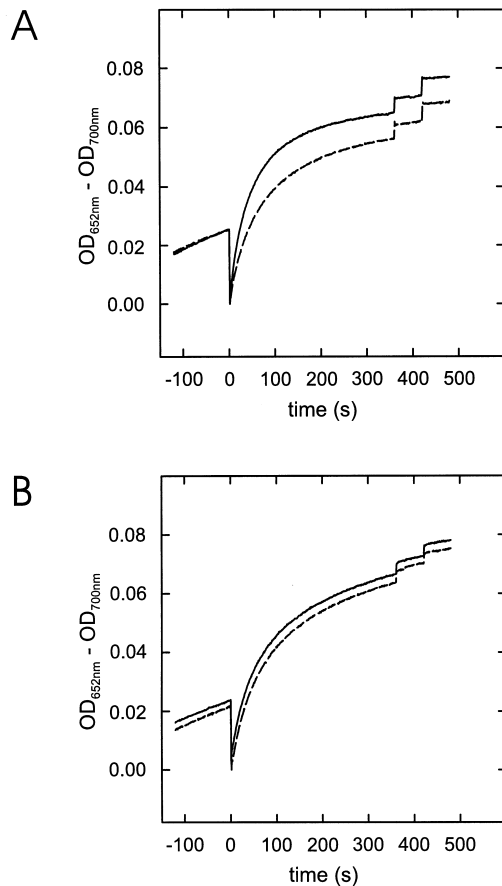


Fig. 6. Partial proteolysis with trypsin activates the Na/Ca-K exchanger in ROS membrane vesicles, but not in proteoliposomes. In both A and B, Ca-release upon addition of 67.6 mM Na at time zero is shown; this Na-concentration results in about half-maximal activation of the exchanger. (For the undershoot upon Na-addition, see legend of Fig. 2.) (A) Incubation of the ROS membrane vesicles for 1 h in 1  $\mu$ g trypsin/ml at 25°C results in a marked enhancement of ROS membrane vesicles (solid line) as compared to control ROS membrane vesicles (dashed line). Note the difference in the initial Ca-fluxes upon addition of Na. (B) In contrast, the same treatment carried out with proteoliposomes virtually does not affect the Na-induced Ca-release. The recording of Ca-release from the trypsin-treated proteoliposomes (solid line) is almost congruent with that of the non-treated proteoliposomes (dashed line), and for clarity, has been shifted by 0.003 OD units. For calibration of the Ca-signals, two additions of 2  $\mu$ l of 1 mM  $CaCl_2$  were injected at the end of each Ca-flux experiment.

proteoliposomes are indistinguishable. In contrast to proteoliposomes, partial proteolysis of membrane vesicles results in a distinct enhancement of the exchanger activity (Fig. 6A).

The dependence of the initial Ca-flux on the Na

concentration added is shown in Fig. 7. The values of both trypsin-treated and non-treated proteoliposomes are virtually undistinguishable (Fig. 7B). The difference between the maximal initial Ca-fluxes of  $3.77 \pm 0.28$  and  $3.47 \pm 0.35$  nmol/s per mg for control and trypsin-treated proteoliposomes, respectively, is statistically insignificant. For ROS membrane vesicles, on the other hand, partial trypsinization

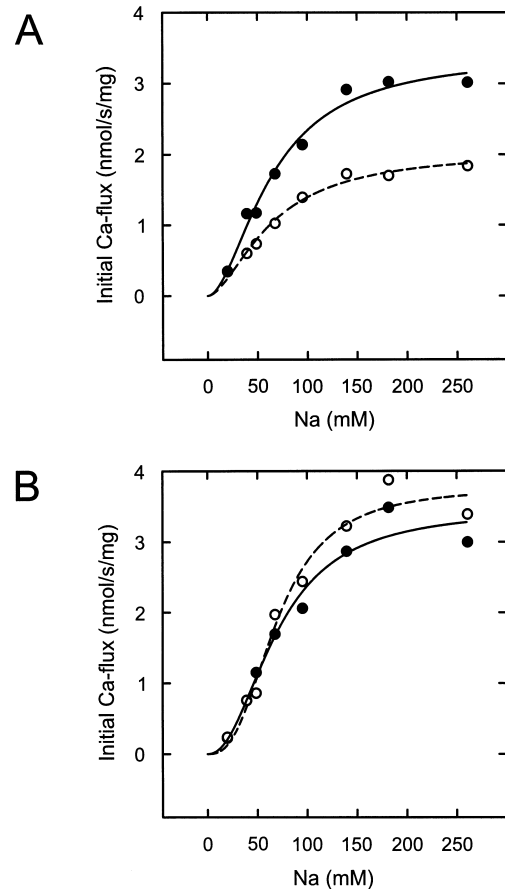


Fig. 7. Na-dependence of the Na/Ca-K exchange with and without partial trypsinization. (A) For ROS membrane vesicles, the initial Na-induced Ca-fluxes were about 70% greater after partial trypsinization (●) as compared to control membranes (○); the maximal initial Ca-fluxes obtained by a Hill curve fit were  $3.40 \pm 0.27$  and  $2.05 \pm 0.15$  nmol/s per mg for trypsin-treated and control membrane vesicles, respectively. (B) For ROS proteoliposomes, however, there is virtually no difference between trypsin-treated (●) and non-treated proteoliposomes (○) observed. The difference of the asymptote values of  $3.47 \pm 0.35$  nmol/s per mg of trypsinized proteoliposomes and  $3.77 \pm 0.28$  nmol/s per mg of control proteoliposomes is not statistically significant. The fitted Hill curves to the data of the trypsin-treated and control samples are shown as solid and dashed lines, respectively.

leads to an enhancement of the Na-induced Ca-fluxes of about 70% as compared to control membrane vesicles (Fig. 7A). Furthermore, the maximal exchange rate of the exchanger in partially proteolyzed ROS membrane vesicles is almost identical to the activity of the exchanger when reconstituted into liposomes.

Averaging several similar experiments, the ratio of the maximal Na-induced Ca-fluxes of trypsin-treated and non-treated exchanger was  $1.75 \pm 0.07$  ( $n=4$ ) for ROS membrane vesicles. In contrast, for trypsin-treated and non-treated ROS proteoliposomes, the ratio of the maximal Na-induced Ca-fluxes was  $0.962 \pm 0.055$  ( $n=3$ ), indicating no statistically significant enhancement of the activity of the exchanger upon partial proteolysis by trypsin.

## 4. Discussion

### 4.1. Regulation of exchange activity by intermolecular interaction

Previously, we demonstrated that the Na/Ca-K exchange molecules exist as dimers in ROS plasma membranes [1]. Here, we report two different approaches to enhance the exchange activity: either (a) by increasing the intermolecular distance of the exchanger dimer with thiol-specific cross-linking reagents, or (b) by proteolytically removing an inhibitory protein domain of the exchanger. Remarkably, the latter mechanism was observed only for the dimerized exchanger suggesting that this inhibitory domain is close to the contact site of the exchanger dimer. Thus, both mechanisms appear to depend on the existence of an exchanger dimer.

The primary indication that the interaction of the exchanger plays a functional role was inferred from thiol-specific cross-linking of the exchanger. Only one or two cross-links per dimer probably form, due to the paucity of cysteines in the amino acid sequence of the Na/Ca-K exchanger [24]. Nevertheless, thiol-specific cross-linking of exchangers to form dimers is quite effective.

Alkylation of the cysteines of the Na/Ca-K exchanger with NEM abated the maximal Ca transport rate by about 20%. In contrast, cross-linking with dimaleimides generally enhanced the transport rate.

The enhancement of the transport rate was correlated with the length of the spacer arm, indicating that this effect was due to an increase of the intermolecular distance of the exchanger dimer. Compared with the NEM modified exchanger, the maximal enhancement of the transport rate was about 50%. Assuming that about half of the exchanger molecules were cross-linked, we estimate that the maximal enhancement of the transport rate of each cross-linked exchanger was about a factor of two.

Changing the intramolecular distance with cross-linking reagents of different sizes is an unusual approach, because cross-linkers are believed to react only when the distance of the reactive amino side chains matches exactly the size of the reagent. For this reason, these compounds are generally considered to constitute ‘molecular rulers’ [28]. However, we found similar cross-linking efficiencies for various dimaleimides that differed considerably in the distance of the reactive groups, indicating that the distance between the neighboring cysteines of adjacent exchanger molecules fluctuates considerably, presumably due to thermal motion. There may be also some flexibility of the spacer arms. On the other hand, the finding reported here that the enhancement of the transport rate correlated with the size of the cross-linker (Fig. 5) suggests that flexibility of the spacer arms has only a minor effect.

Another line of evidence for a regulatory role of the exchanger dimer was derived from both partial proteolysis and functional reconstitution of the exchanger. If the monomers within a dimer exert a self-inhibitory influence on each other, then the monomeric exchanger should be more active than the dimeric exchanger of the ROS plasma membrane. Previously, we reported evidence that the Na/Ca-K exchanger is monomeric after reconstitution into proteoliposomes [1]. The transport rate of the exchanger after solubilization and reconstitution into lipid vesicles was in fact about twice as active as the exchanger in the ROS plasma membrane. We infer from this study that this finding, which had been reported earlier [29], is probably due to the fact that there is no mutual inhibition of the exchanger because the exchangers exist only as monomers in this preparation.

Partial proteolysis of ROS membrane vesicles also

led to a two-fold enhancement of the transport rate of the exchanger, in agreement with earlier reports [21,22]. An inhibitory protein region could be proteolytically removed; however, the mechanism of this inhibition has not been revealed. We show here that proteolytic activation of the exchanger is observed only in the dimerized exchanger, suggesting that the contacting protein domains of the exchanger molecules regulate the exchange activity.

Proteolytic activation has also been reported for the cardiac Na–Ca exchanger and other Na–Ca exchangers [20–22,30]. For the cardiac Na–Ca exchanger an inhibitory 20-amino-acid peptide, XIP, has been identified on the intracellular loop [23,31,32]. However, in the amino acid sequence of the Na/Ca-K exchanger, no protein domain homologous to the XIP peptide has been identified [24].

#### 4.2. Maximal Ca-transport rate of the Na/Ca-K exchanger

Based on the maximal Ca exchange flux of  $0.059 \pm 0.012$  mol  $\text{Ca}^{2+}/\text{s}$  per mol Rh (see Section 3), an estimate of the maximal Ca transport rate of the exchanger can be obtained. The Na/Ca-K exchanger and the cGMP-gated channels are both exclusively localized in the plasma membrane of the ROS [7–9]. Moreover, previous results indicated that the Na/Ca-K exchanger is bound to the cGMP-gated channel in a stoichiometric ratio of two exchangers per one channel [2]. For bovine ROS, the channel density in the plasma membrane has been estimated to be 260 channels/ $\mu\text{m}^2$ , or one channel per 1560 rhodopsin molecules [14]. Taking these pieces of information together, there is one exchanger molecule per 780 rhodopsin molecules in bovine ROS membranes. The maximal Na-induced Ca flux of ROS membrane vesicles can thus be converted into an average maximal transport rate per exchanger molecule of  $46.1 \pm 9.7$   $\text{Ca}^{2+}/\text{s}$ . This transport rate has still to be corrected for the presence of both normal and reversed Na/Ca-K exchange because the ROS membrane vesicles comprise both outside-out and inside-out vesicles in about equal frequency [14]. The normal Na/Ca-K exchange has previously been found to be about twice as great as the reversed Na/Ca-K exchange [29]. Therefore, we estimate for the normal mode Na/Ca-K exchange in

bovine ROS a maximal transport rate of about 60  $\text{Ca}^{2+}/\text{s}$  per exchanger.

This value is greater than the value estimated by Hodgkin et al. for the exchanger in salamander ROS [33], and similar to the value estimated for the Na–Ca exchanger of the exoskeletal muscle of the lobster [30], but almost two orders of magnitude smaller than the Ca flux estimated for the cardiac Na–Ca exchanger [34–36].

#### 4.3. Ca-permeability due to Na/Ca-K exchange

The initial Ca flux is directly dependent on the transport rate of the exchanger, and is not influenced by the geometry of the vesicles (see Section 2). Therefore, this quantity can be used to estimate the transport rate of the exchanger (see above). Moreover, the increase of the Na-dependent Ca-permeability can be estimated with Eq. 10 if the mean vesicle diameter is known. Because the vesicles were prepared by extrusion through a 0.4- $\mu\text{m}$  Nuclepore filter, we assume a mean vesicle diameter of 0.4  $\mu\text{m}$ . With this value we obtain an increase of the Ca-permeability  $P$  of  $7.5 \times 10^{-4}$   $\mu\text{m}/\text{s}$  upon maximal Ca activation of the exchanger.

However, the efflux kinetics is generally not single-exponential due to heterogeneity of vesicle sizes. For this reason, multiphasic Ca efflux kinetics from a vesicle preparation do not necessarily indicate different activation states.

#### 4.4. Local Ca-signaling in rod outer segments?

Local Ca microdomains are generally encountered near a single Ca channel [37]. The association of cGMP-gated channel and Na/Ca-K exchanger in rod photoreceptors [2,14] suggests a different way to restrict a Ca signal to the close vicinity of the channel, as will be discussed in the next paragraph. Therefore, it seems plausible that the guanylate cyclase, the main Ca sensor of photoreceptors, and possibly other proteins of the transduction cascade as well, are close to the channel. However, although peptides of the glutamic acid rich protein domain of the channel  $\beta$ -subunit have been reported to bind the guanylate cyclase and other proteins [38], a direct binding of the guanylate cyclase to the channel could not be confirmed [39]. The cGMP-gated chan-

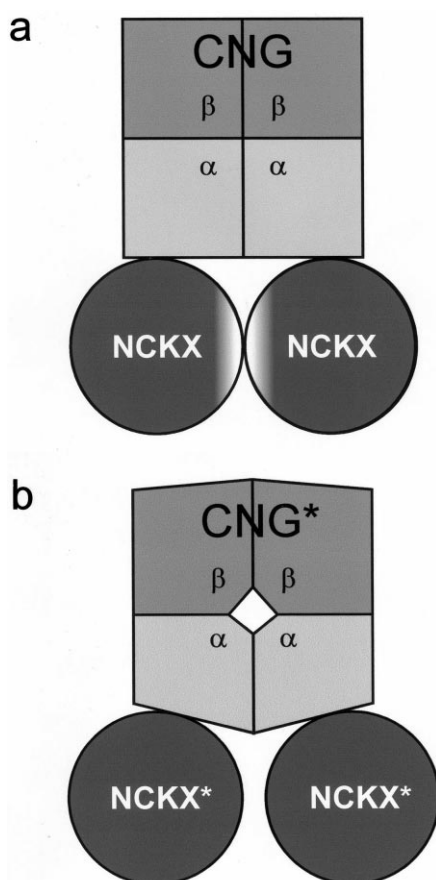


Fig. 8. Hypothetical regulatory mechanism of Na/Ca-K exchange in the channel-exchanger complex of photoreceptors (CNG, cyclic nucleotide gated channel; NCKX, Na/Ca-K exchanger): (a) at closed cGMP-gated channel, the interacting inhibitory domains (light-gray areas) of the exchanger dimer abate the exchanger activity; (b) activation of the cGMP-gated channel leads to an increase of the exchange activity by increasing the intermolecular distance of the associated exchanger dimer (the star signifies activation). The results reported in this study suggest that increasing the intermolecular distance of the exchanger molecules by only a few angstroms would be sufficient to elevate the exchanger activity markedly. The depicted subunit arrangement of the channel is supported by two recent studies [2,42]; however, He et al. propose the subunit arrangement  $\alpha$ - $\beta$ - $\alpha$ - $\beta$  for the native cGMP-gated channel of the photoreceptor [43].

nel is anchored to peripherin, an integral protein of the disc rim [39]. The localization of the guanylate cyclase relative to the channel remains to be elucidated.

A necessary condition for local Ca signaling required by mass conservation is that the Ca influx through the channel is balanced by an equal Ca ef-

flux through the exchanger. The following estimation shows that this is the case for rod photoreceptors of amphibians. The plasma membrane area of frog rod photoreceptors is about  $1200 \mu\text{m}^2$ , and the dark current is 25 pA [40]. Assuming a mean channel density of 650 channels/ $\mu\text{m}^2$  [41], and considering that 15% of the dark current is due to Ca influx [15], we obtain a Ca flux of  $15 \text{ Ca}^{2+}/\text{s}$  per channel under physiological conditions. This value is indeed smaller than the maximal Ca export rate per exchanger molecule estimated by Hodgkin et al. [33].

For mammalian photoreceptors, the magnitude of the Ca influx is likely to be similar to this value, and the activity of the two exchangers associated with the channel is far from saturation as well. Therefore, the existence of a channel-exchanger complex and the results reported here suggest that activation of the channel possibly leads to an increase of the exchanger activity by reducing the inhibitory interaction between the exchanger dimer (Fig. 8). Such an allosteric mechanism would contribute to restrict the Ca signal to the close vicinity of the channel because the rate of Ca extrusion would be increased when the channel is activated and Ca enters the cell.

## Acknowledgements

We thank Dr. Jeffrey W. Karpen, B.Sc., Andrew Mahoney, and Dr. Paul P.M. Schnetkamp for comments on the manuscript. We also thank Dr. Robert S. Molday for providing the monoclonal antibody PMe 1B3 against the retinal Na/Ca-K exchanger, and Dr. Volker Hagen for synthesizing BMP. This work was supported by a grant of the Deutsche Forschungsgemeinschaft (Ba 721/1-3).

## References

- [1] A. Schwarzer, T.S.Y. Kim, V. Hagen, R.S. Molday, P.J. Bauer, The Na/Ca-K exchanger of rod photoreceptor exists as dimer in the plasma membrane, *Biochemistry* 36 (1997) 13667–13676.
- [2] A. Schwarzer, H. Schauff, P.J. Bauer, Binding of the cGMP-gated channel to the Na/Ca-K exchanger in rod photoreceptors, *J. Biol. Chem.* 275 (2000) 13448–13454.
- [3] A.L. Hodgkin, Modulation of ionic currents in vertebrate

- photoreceptors, *Proc. Retina Res. Found. Symp.* 1 (1988) 6–30.
- [4] P.A. McNaughton, Light response of vertebrate photoreceptors, *Physiol. Rev.* 70 (1990) 847–883.
  - [5] K.-W. Yau, Phototransduction mechanism in retinal rods and cones, *Invest. Ophthalmol. Vis. Sci.* 35 (1994) 9–32.
  - [6] W.N. Zagotta, S.A. Siegelbaum, Structure and function of cyclic nucleotide-gated channels, *Annu. Rev. Neurosci.* 19 (1996) 235–263.
  - [7] P.J. Bauer, Evidence for two functionally different membrane fractions in bovine retinal rod outer segments, *J. Physiol. (Lond.)* 401 (1988) 309–327.
  - [8] N.J. Cook, L.L. Molday, D. Reid, U.B. Kaupp, R.S. Molday, The cGMP-gated channel of bovine rod photoreceptors is localized exclusively in the plasma membrane, *J. Biol. Chem.* 264 (1989) 6996–6999.
  - [9] D.M. Reid, U. Friedel, R.S. Molday, N.J. Cook, Identification of the sodium-calcium exchanger as the major ricin-binding glycoprotein of bovine rod outer segments and its localization to the plasma membrane, *Biochemistry* 29 (1990) 1601–1607.
  - [10] S.E. Gordon, W.N. Zagotta, Subunit interactions in coordination of  $\text{Ni}^{2+}$  in cyclic nucleotide-gated channels, *Proc. Natl. Acad. Sci. USA* 92 (1995) 10222–10226.
  - [11] M.D. Varnum, W.N. Zagotta, Subunit interactions in the activation of cyclic nucleotide-gated ion channels, *Biophys. J.* 70 (1996) 2667–2679.
  - [12] D.T. Liu, G.R. Tibbs, S.A. Siegelbaum, Subunit stoichiometry of cyclic nucleotide-gated channels and effects of subunit order on channel function, *Neuron* 16 (1996) 983–990.
  - [13] M.L. Ruiz, J.W. Karpen, Single cyclic nucleotide-gated channels locked in different ligand-bound states, *Nature* 389 (1997) 389–392.
  - [14] P.J. Bauer, M. Drechsler, Association of cyclic GMP-gated channels and  $\text{Na}^+/\text{Ca}^{2+}/\text{K}^+$  exchangers in bovine retinal rod outer segment plasma membranes, *J. Physiol. (Lond.)* 451 (1992) 109–131.
  - [15] K. Nakatani, K.-W. Yau, Calcium and magnesium fluxes across the plasma membrane of the toad rod outer segment, *J. Physiol. (Lond.)* 395 (1988) 695–729.
  - [16] U.B. Kaupp, K.-W. Koch, Role of cGMP and  $\text{Ca}^{2+}$  in vertebrate photoreceptor excitation and adaptation, *Annu. Rev. Physiol.* 54 (1992) 153–175.
  - [17] P.P.M. Schnetkamp, R.T. Szerencsei, Intracellular  $\text{Ca}^{2+}$  sequestration and release in intact bovine retinal rod outer segments, *J. Biol. Chem.* 268 (1993) 12449–12457.
  - [18] G.L. Fain, W.H. Schröder, Calcium content and calcium exchange in dark-adapted toad rods, *J. Physiol. (Lond.)* 368 (1985) 641–665.
  - [19] A.P. Somlyo, B. Walz, Elemental distribution in *Rana pipiens* retinal rods: Quantitative electron probe analysis, *J. Physiol.* 358 (1985) 183–195.
  - [20] P.J. Bauer, H. Schauf, A. Schwarzer, J.E. Brown, Direct evidence of  $\text{Na}^+/\text{Ca}^{2+}$  exchange in squid rhabdomeric membranes, *Am. J. Physiol.* 276 (1999) C558–C565.
  - [21] D.A. Nicoll, B.R. Barrios, K.D. Philipson,  $\text{Na}^+/\text{Ca}^{2+}$  exchangers from rod outer segments and cardiac sarcolemma: comparison of properties, *Am. J. Physiol.* 260 (1991) C1212–C1216.
  - [22] T.S.Y. Kim, D.M. Reid, R.S. Molday, Structure-function relationships and localization of the  $\text{Na}/\text{Ca}/\text{K}$  exchanger in rod photoreceptors, *J. Biol. Chem.* 273 (1998) 16561–16567.
  - [23] Z. Li, D.A. Nicoll, A. Collins et al., Identification of a peptide inhibitor of the cardiac sarcolemmal  $\text{Na}^+/\text{Ca}^{2+}$  exchanger, *J. Biol. Chem.* 266 (1991) 1014–1020.
  - [24] H. Reiländer, A. Achilles, U. Friedel, G. Maul, F. Lottspeich, N.J. Cook, Primary structure and functional expression of the  $\text{Na}/\text{Ca}/\text{K}$ -exchanger from bovine rod photoreceptors, *EMBO J.* 11 (1992) 1689–1695.
  - [25] P.J. Bauer, H. Schauf, Self-inhibition of the  $\text{Na}/\text{Ca}/\text{K}$  exchanger in rod photoreceptors, *Biophys. J.* 80 (2001) 20a.
  - [26] R.S. Kaplan, P.L. Pedersen, Determination of microgram quantities of protein in the presence of milligram levels of lipid with Amido Black 10B, *Anal. Biochem.* 150 (1985) 97–104.
  - [27] P.J. Bauer, Affinity and stoichiometry of calcium binding by arsenazo III, *Anal. Biochem.* 110 (1981) 61–72.
  - [28] S.S. Wong, *Chemistry of Protein Conjugation and Cross-linking*, CRC Press, Boca Raton, FL, 1991.
  - [29] B. Huppertz, P.J. Bauer,  $\text{Na}^+/\text{Ca}^{2+}/\text{K}^+$  exchange in bovine retinal rod outer segments: quantitative characterization of normal and reversed mode, *Biochim. Biophys. Acta* 1189 (1994) 119–126.
  - [30] A. Eisenrauch, M. Juhaszova, M.P. Blaustein, Regulatory processes on the cytoplasmic surface of the  $\text{Na}^+/\text{Ca}^{2+}$  exchanger from lobster exoskeletal muscle, *J. Membr. Biol.* 174 (2000) 225–235.
  - [31] Z. He, N. Petesch, K.-P. Voges, W. Rösen, K.D. Philipson, Identification of important amino acid residues of the  $\text{Na}^+/\text{Ca}^{2+}$  exchanger inhibitory peptide, XIP, *J. Membr. Biol.* 156 (1997) 149–156.
  - [32] S. Matsuoka, D.A. Nicoll, H. Zhaoping, K.D. Philipson, Regulation of the cardiac  $\text{Na}^+/\text{Ca}^{2+}$  exchanger by the endogenous XIP region, *J. Gen. Physiol.* 109 (1997) 273–286.
  - [33] A.L. Hodgkin, P.A. McNaughton, B.J. Nunn, Measurement of sodium-calcium exchange in salamander rods, *J. Physiol. (Lond.)* 391 (1987) 347–370.
  - [34] E. Niggli, W.J. Lederer, Molecular operations of the sodium-calcium exchanger revealed by conformation currents, *Nature* 349 (1991) 621–624.
  - [35] D.W. Hilgemann, Unitary cardiac  $\text{Na}^+/\text{Ca}^{2+}$  exchange current magnitudes determined from channel-like noise and charge movements of ion transport, *Biophys. J.* 71 (1996) 759–768.
  - [36] M. Kappl, K. Hartung, Rapid charge translocation by the cardiac  $\text{Na}^+/\text{Ca}^{2+}$  exchanger after a  $\text{Ca}^{2+}$  concentration jump, *Biophys. J.* 71 (1996) 2473–2485.
  - [37] P.J. Bauer, The local Ca concentration profile in the vicinity of a Ca channel, *Cell Biochem. Biophys.* 35 (2001) 49–61.
  - [38] H.G. Körschen, M. Beyermann, F. Müller et al., Interaction of glutamic-acid-rich proteins with the cGMP signalling pathway in rod photoreceptors, *Nature* 400 (1999) 761–766.

- [39] A. Poetsch, L.L. Molday, R.S. Molday, The cGMP-gated channel and related glutamic acid rich proteins interact with peripherin-2 at the rim region of rod photoreceptor disc membranes, *J. Biol. Chem.* 276 (2001) 48009–48016.
- [40] L. Stryer, Cyclic GMP cascade of vision, *Annu. Rev. Neurosci.* 9 (1986) 87–119.
- [41] J.W. Karpen, D.A. Loney, D.A. Baylor, Cyclic GMP-activated channels of salamander retinal rods: spatial distribution and variation of responsiveness, *J. Physiol. (Lond.)* 448 (1992) 257–274.
- [42] I.M. Shammat, S.E. Gordon, Stoichiometry and arrangement of subunits in rod cyclic nucleotide-gated channels, *Neuron* 23 (1999) 809–819.
- [43] Y. He, M.L. Ruiz, J.W. Karpen, Constraining the subunit order of rod cyclic nucleotide-gated channels reveals a diagonal arrangement of like subunits, *Proc. Natl. Acad. Sci. USA* 97 (2000) 895–900.